Journal of Geography, Environment and Earth Science International

Volume 29, Issue 11, Page 27-48, 2025; Article no.JGEESI.145402
ISSN: 2454-7352

Topographic and Radiometric Integration for Enhanced Structural Mapping in Gold Exploration: A Case Study of North Central Nigeria

Lawrence Jane Osita [a*], Abu Mallam [b], Nasir Naeem Abdulsalam [b] and Gajere Jiriko Nzeghi [c]

[a] Department of Geophysics, Federal University of Technology, Minna, Nigeria.
[b] Department of Physics, University of Abuja, Abuja, Nigeria.
[c] Department of Geology and Mining, University of Abuja, Abuja, Nigeria.

Authors' contributions

This work was carried out in collaboration among all authors. Author LJO managed the literature searches, analyzed the data, and wrote the manuscript. Authors AM, NNA and GJN designed the study, checked the protocol of the study, the grammar and language, and appraised data quality. All authors read and approved the final manuscript.

Article Information

DOI: https://doi.org/10.9734/jgeesi/2025/v29i11966

Open Peer Review History:
This journal follows the Advanced Open Peer Review policy. Identity of the Reviewers, Editor(s) and additional Reviewers, peer review comments, different versions of the manuscript, comments of the editors, etc are available here: https://pr.sdiarticle5.com/review-history/145402

Original Research Article

Received: 10/08/2025
Published: 22/10/2025

ABSTRACT

Accurate delineation of structurally controlled hydrothermal alteration zones is critical for gold exploration in basement terrains. This study integrates topographic and radiometric data to enhance structural mapping in parts of North-Central Nigeria, a region within the Nigerian Basement Complex known for gold mineralization. Shuttle Radar Topography Mission (SRTM) data and radiometric datasets were processed to delineate lineaments, identify hydrothermal alteration

**Corresponding author: E-mail: jane.osita@futminna.edu.ng, janelaw09@gmail.com;*

Cite as: *Lawrence Jane Osita, Abu Mallam, Nasir Naeem Abdulsalam, and Gajere Jiriko Nzeghi. 2025. "Topographic and Radiometric Integration for Enhanced Structural Mapping in Gold Exploration: A Case Study of North Central Nigeria". Journal of Geography, Environment and Earth Science International 29 (11):27–48. https://doi.org/10.9734/jgeesi/2025/v29i11966.*

zones, and establish their relationship with known gold occurrences. Topographic derivatives such as slope, curvature, aspect, and terrain ruggedness Index (TRI) were combined with potassium (K), thorium (Th), and uranium (U) concentration maps, as well as K/Th and F-parameter ratios, to highlight regions of structural complexity and potential mineralization. Lineament density and directional analyses revealed dominant NE-SW and NW-SE structural trends, consistent with regional tectonics, which coincide with mapped gold mineralized zones, suggesting strong tectonic controls on mineral emplacement. Results indicate that potassium anomalies, elevated K/Th ratios, and high F-parameter values are spatially in line with structurally controlled zones delineated from topographic analysis. Several of these coincident anomalies correspond to known artisanal gold mining sites, while others define previously unrecognized prospective corridors. This investigation demonstrates how the fusion of SRTM-derived geomorphological parameters and airborne radiometric data helps improve the delineation of gold favourable zones. The findings contribute to exploration strategies by delineating priority zones that warrant detailed geophysical and geochemical follow-up.

Keywords: Topography; radiometric; gold exploration; structural mapping; North Central Nigeria.

1. INTRODUCTION

The search for mineral resources, especially gold, in complex geological terrains such as North Central Nigeria necessitates integration of multi-source techniques. Hydrothermal alteration zones are key exploration targets for these gold mineral deposits. These zones often occur along structurally controlled pathways (Ekwok *et al.,* 2024) and are associated with variations in physical and geochemical properties detectable through geophysical and radiometric methods. These alteration regions are often associated with shear zones (Ramadan & Abdelfattah, 2010), brittle–ductile deformations (Ebele *et al*., 2021), and fracture networks. Hydrothermal alteration processes typically produce mineralogical and geochemical changes in host rocks, leading to detectable variations in potassium (K), thorium (Th), and uranium (U) concentrations (Akinlalu, 2023). These variations can be captured effectively using airborne radiometric surveys, which provide spatially continuous measurements of gamma-ray emissions from natural radioelements (Akinlalu, 2023).

In mineralized systems, potassic enrichment is often associated with sericitization, K-feldspar alteration, and illitization, while depletion of thorium and uranium may result from mobilization during hydrothermal fluid flow (Akinlalu, 2023; Eldosouky *et al.,* 2024). Radiometric ratio maps such as Th/K and ternary (K–Th–U) composites, together with derived indices such as the K-deviation (K_d) and the F-parameter, are effective tools for highlighting hydrothermal-alteration footprints; when integrated with structural datasets, these radiometric signatures have been shown to delineate alteration halos and prospective mineralized zones in basement terrains (Sanusi & Amigun, 2020; Akinlalu, 2023; Salako *et al.,* 2024).

Traditional structural mapping, based solely on geophysical or geological observations, may overlook subtle topographic and geochemical indicators of mineralization (Hronsky & Groves, 2008). Sanusi and Amigun (2020) analyzed airborne magnetic and gamma-ray spectrometry data along the Paiko–Abaji axis, covering areas such as Gurara and Izom within the Kushaka Schist Belt of North-central Nigeria, to evaluate subsurface structures and hydrothermal alteration halos linked to orogenic gold mineralization. Similarly, Saleh *et al*. (2022) integrated aeromagnetic and radiometric datasets to map structural features associated with gold mineralization around Minna, revealing dominant NE–SW and NW–SE lineament trends that mirror the tectonic influence of the Pan-African orogeny. However, both studies placed limited emphasis on subtle topographic expressions that could further indicate zones of mineralization.

The integration of airborne radiometric data with digital elevation model (DEM)-derived terrain attributes such as slope, curvature, ruggedness index, and topographic position index (TPI) can enhance alteration mapping by providing additional structural and geomorphological context. Recent advances in geospatial integration have demonstrated the effectiveness of combining geophysical, remote sensing, and topographic datasets for alteration mapping and mineral prospectivity analysis. Frutuoso *et al.*

(2021) demonstrated the effectiveness of using remote sensing data in detecting hydrothermal alteration zones linked to gold mineralization in northern Portugal. Similarly, Sheikhrahimi *et al.* (2019) employed ASTER imagery in Iran to showcase the capability of remote sensing techniques in mapping mineralization patterns with high spatial accuracy and geological relevance. Studies in Africa, such as those of Anaba Fotze *et al.* (2022) and Eldosouky *et al.* (2024), affirmed the reliability and applicability of integrating satellite imagery with geophysical data in exploring for minerals. In Nigeria, Ohwo & Fadeyi (2024) integrated airborne radiometric indices with structural mapping derived from remote sensing and topographic datasets in the Igarra Schist Belt and delineated prospective corridors for gold mineralization. These studies proved the effectiveness of integrating multi-source datasets in enhancing the delineation of hydrothermal alteration zones and potential mineralized areas, particularly when employing techniques such as radiometric indices and terrain derivative analysis.

This study adopts such an integrated approach to map hydrothermal alteration zones in North-Central Nigeria by fusing airborne radiometric datasets (K, Th, U, Th/K, K-deviation, F-parameter, and ternary composites) with DEM-derived terrain attributes. The objective is to identify structurally controlled alteration belts that could serve as exploration targets for gold mineral deposits.

1.1 Location, Geology, and Topography of the Study Area

The research area is bounded by latitude 8°30'00"– 10°00'00" North and longitude 5°00'00"– 9°00'00" East. The study area (72,600 square kilometers) encompasses parts of Niger state, the Federal Capital Territory (FCT), and a few other towns in Kaduna, Plateau, and Nasarawa adjoining the FCT. The study area comprises approximately 7.86% of Nigeria's landmass and is part of the North Central geopolitical zone.

The study area mainly lies within the Nigerian Basement Complex (Fig. 1). This region is part of the Pan-African mobile belt, bordered by the West African Craton to the west and the Congo Craton to the southeast (Ominigbo, 2022). It represents a tectonically active zone characterized by multiple deformation events, intense metamorphism, and magmatic intrusions (Rahaman, 1988; Ajibade et al., 2008). Geologically, the area is underlain by a wide variety of lithologies, including gneisses, granites, and metavolcanic sequences or Pan-African granitoids (Rahaman, 1988; Obaje, 2009; Lukman et al., 2024; Lawrence et al., 2025). Generally, the region is mainly underlain by Precambrian basement rocks consisting of geologic units such as migmatite, migmatitic gneiss, granite gneiss, porphyritic granite, granite and granite porphyry, biotite granite, and undifferentiated schist (Fig. 2). These rocks have been extensively reworked during the Pan-African orogeny (~600–500 Ma), which played a significant role in the tectonic and lithological evolution of the area (Obaje, 2009). The schist belts, located within the Nigerian Basement Complex (Precambrian), are said to host most of the economic minerals (Akintola & Adekeye, 2008). These belts are Proterozoic in age and consist of metasedimentary (Chinwuko et al., 2019) and metavolcanic rocks, which have been intruded by syn- to post-tectonic granitoids (Obaje, 2009). These schist belts are known for their high mineral potential, particularly for gold, base metals, and rare minerals, making them strategic targets for exploration.

Structurally, the terrain is dominated by NE-SW and NW-SE trending shear zones, fractures, and faults, as documented by researchers such as Ogunmola *et al*. 2015, Abraham *et al.* (2024), and Lawrence *et al.* (2025), which serve as major conduits for hydrothermal fluids responsible for gold mineralization (Abraham *et al.*, 2024). These structures reflect the Pan-African orogenic processes, which reactivated pre-existing basement fabrics, creating dilation zones that are favourable for fluid flow and ore deposition (Akinluyi *et al.,* 2021). In addition to the structural framework, the region exhibits evidence of hydrothermal alteration, associated with artisanal and small-scale mining activities within Minna and Paiko districts, as well as Pangu, Wuna, and Chechey districts, as documented by Ayuba and Abu (2024), confirming the economic potential of these zones. Hydrothermal zones are commonly marked by potassic alteration, silicification, and ferruginization, which are reflected in both the radiometric datasets (potassium and Th/K anomalies) and in geophysical signatures such as gravity lows and magnetic disruptions (Abdelrady *et al.,* 2023; Saleh *et al.,* 2022).

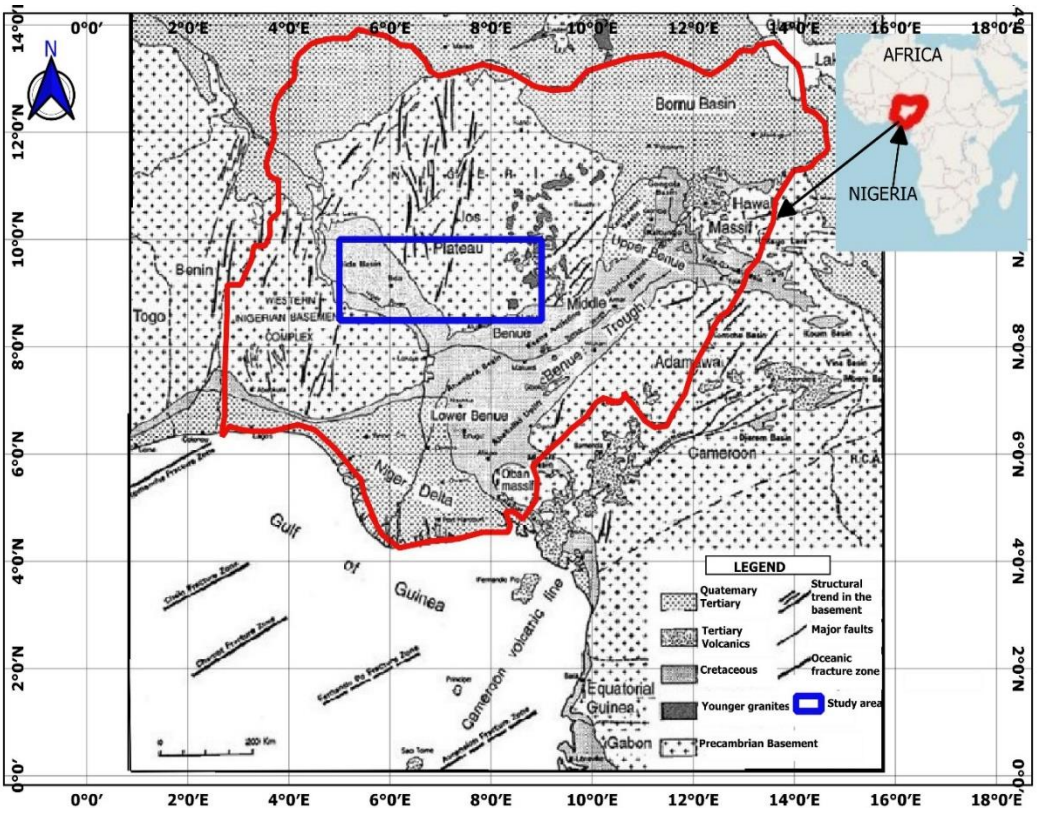

Fig. 1. The Geological map of Nigeria showing the Precambrian basement complex, the sedimentary basins, and the study location; Modified after Ayoola *et al.* (2019)

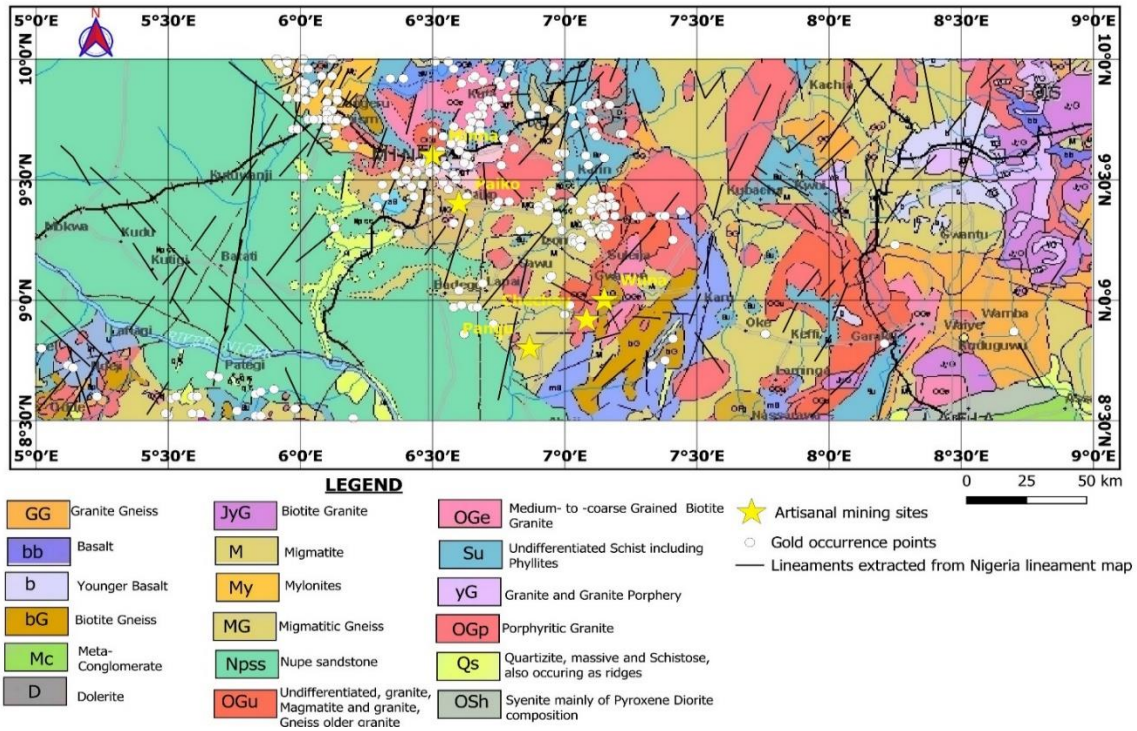

Fig. 2. The geological map of the study area (Extracted from NGSA 2023a) superimposed with lineaments, gold occurrence zones, and artisanal mining sites

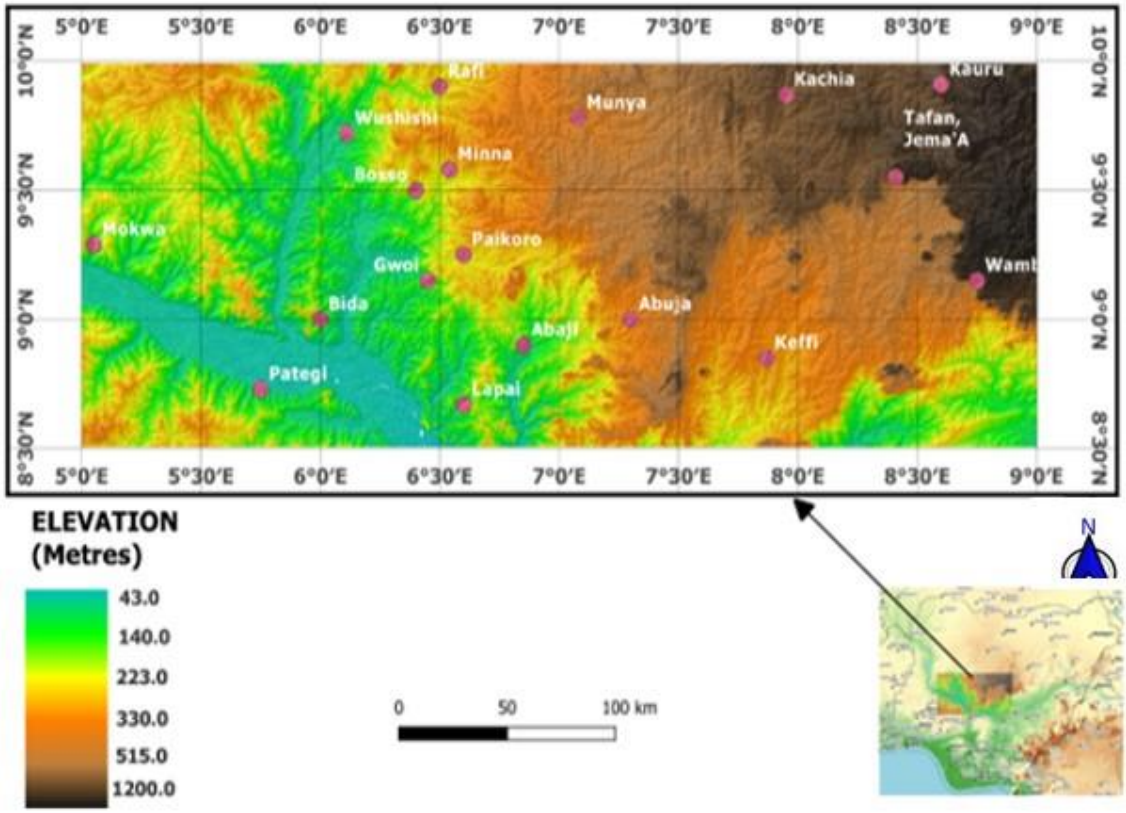

Fig. 3. Topography map for the study area [Extracted from USGS Earth Explorer website: https://earthexplorer.usgs.gov/ on June 5th, 2024; Modified using free and open source QGIS software]

The Topography of the study area (Fig. 3) is characterized by pen plains with a relatively flat landscape and gentle slopes, particularly around Bida and Pategi, as the flanks of the River Niger deposit sediments in this region. Northeast of the study area, in towns like Minna, Abuja, Kachia, Wamba, Jema'a, the topography is seen to be high, ranging from an average elevation of 400 m to about 1500 m. The residents within this region are predominantly Gwari, Nupe, Jabba, Kagoma, and Koro, with farming, trading, and cattle rearing as their main occupations.

2. MATERIALS AND METHODS

2.1 Data Acquisition

This study utilized both radiometric and topographic datasets to identify structural controls and hydrothermal alteration zones related to gold mineralization in North-Central Nigeria. Twenty-four (24) high-resolution airborne radiometric datasheets were obtained from the Nigerian Geological Survey Agency (NGSA) as grid multichannel datasheets of potassium (K), Thorium (Th), and Uranium (U). The sheets are Fashe (161), Akerre(162), Zungeru (163), Minna (164), Bishini (165), Kachia (166), Kafanchan (167), Naragatu 168), Mokwa (182), Egbako (183), Bida (184), Paiko (185), Abuja (186), Gitata (187), Jema'a (188), Kurra (189), Lafiagi (203), Pategi (204), Baro (205), Gulu (206), Kuje (207), Keffi (208), Akwanga (209), and Wamba (210). These data were acquired and processed into grids by Fugro Airborne Surveys between 2002 and 2009 for NGSA using 512-channel gamma-ray spectrometers (NaI "Tl" crystals with a size of 2″ × 2″) mounted on fixed-wing aircraft. The radiometric data were obtained along the NW-SE flight line at an average elevation of 100 m, flight spacing of 500 m, and tie lines of 200 m.

Topographic data for the research were derived from the Shuttle Radar Topography Mission (SRTM) digital elevation model (DEM) needed for structural and geomorphological analysis Eight (8) "1 Arc-Second" SRTM data (SRTM1N08E005V3, SRTM1N08E006V3, SRTM1N08E007V3, SRTM1N08E008V3, SRTM1N09E005V3, SRTM1N09E006V3,

SRTM1N09E007V3, and SRTM1N09E008V3) retrieved from https://earthexplorer.usgs.gov/ on June 5th, 2024 on a 30 m resolution were used for this research. The SRTM data were made available online on September 23rd, 2014.

2.2 Data Preprocessing

The composite grid of potassium, thorium, and uranium was obtained by merging the individual radiometric grids using the "grid knitting" tool in Oasis Montaj. Noise filtering was applied to the radiometric grids using low-pass convolution filters to suppress random variations while preserving anomaly patterns (IAEA, 2003).

The eight DEM datasets were first merged using the "build virtual raster" tool in QGIS to produce a composite DEM image from which a subset covering the study area was extracted. The "clip raster by extent" tool was used to extract the study extent from the composite DEM map for further analysis. To ensure spatial consistency, all datasets were projected into a common coordinate reference system (CRS) (EPSG: 32632, WGS 84 / UTM Zone 32N) and processed with a uniform spatial resolution of 30 m to avoid spatial misalignment.

2.3 DEM Data Processing and Lineament Extraction

Geomorphic indices such as slope, aspect, curvature, and terrain ruggedness index were obtained from the DEM composite raster image using the "Raster analysis" tool in QGIS. These indices were necessary to quantify the surface relief and to identify geomorphic anomalies caused by faulting within the study area.

Lineaments were extracted from the DEM composite image using the "Hillshade tool" in QGIS. The hillshade raster was generated after setting the azimuth, altitude, and the Z-factor to 315°, 45°, and 1, respectively, and specifying an output file location. For better visualization and structural interpretation, a multi-directional illumination was applied by generating multiple hillshade rasters at varying azimuths of 315°, 270°, 225°, 135°, and 90°. The lineament digitization was then performed manually by creating a new vector shapefile "gpkg" in QGIS, selecting the "Linestring" geometry type. Employing the "Add Line Feature" tool and activating the editing mode, the visible lineaments on the hillshade images were traced.

2.4 Hydrothermal Alteration Indicators

Radiometric data processing focused on extracting both elemental concentration maps and analytic indicators of mineral deposits such as gold. In radiometric geophysical data analysis, several indicators of hydrothermal alteration can be used to identify potential mineral deposits. The common indicator is the presence of radioelements like potassium, thorium, and uranium. The distribution of these elements can be genetically linked to gold mineralization, often associated with hydrothermal alteration (Sanusi & Amigun, 2020; Olomo *et al*., 2022; Ohwo & Fadeyi, 2024) and can be detected using radiometric techniques such as gamma-ray spectrometry and airborne radiometric surveys (Mamouch *et al*., 2022). Other indicators include thorium-potassium ratio (Th/K), Potassium derivative (K_d), F-Parameter, and ternary.

2.4.1 The ratio maps

The Thorium-to-Potassium (Th/K) ratio map is a crucial radiometric tool for identifying zones of hydrothermal alteration, which are often associated with gold mineralization. This ratio can be used to identify different types of hydrothermal alteration and can be detected using radiometric techniques such as gamma-ray spectrometry and airborne radiometric surveys (Chiozzi *et al.* 2007; Ahmed *et al.,* 2021; Baratoux *et al.,* 2021; Mamouch *et al.,* 2022). The Th/K ratio is computed to highlight potassic alteration zones associated with gold mineralization.

The Potassium-to-Thorium (K/Th) ratio map, which is the inverse of the Th/K map, showcases the geochemical variation between potassium (K) and thorium (Th) concentrations across the study area. The ratio serves as an indicator of hydrothermal alteration. Potassic alteration (Akinlalu 2023) and argillic alteration (Andogma *et al.,* 2020) are significant aspects of hydrothermal alteration, commonly associated with gold mineralization. Thorium is a relatively immobile element during alteration processes, while potassium is often introduced or enriched by hydrothermal fluids. Thus, an elevated K/Th ratio implies possible enrichment of potassium due to metasomatic activity or weathering processes linked to mineralizing systems.

2.4.2 Potassium deviation (K_d)

Potassium deviation (Kd), another hydrothermal indicator, highlights subtle potassium anomalies. Positive K-deviation suggests enrichment of

potassium potentially linked to alteration, while negative values imply relative depletion. Such methods have been successfully applied in Nigerian basement terrains using aero-radiometric datasets (Salako *et al.,* 2024).

Employing the method developed by Saunders *et al*. (1987) and Pires (1995), as documented by Sanusi and Amigun (2020) and Salako *et al.* (2024), deviation from the nominal K values (K_d) represents potassium enrichment values due to hydrothermal alteration processes. The nominal K value (K_n) in relation to the equivalent thorium (Th) can be obtained from equation 1 (De Quadros *et al*., 2003; Sanusi & Amigun, 2020; Salako *et al.,* 2024).

$$K_n = \left(\frac{K\ grid_{average}}{Th\ grid_{average}}\right) \times Th\ Map \quad (1)$$

The potassium deviation (K_d) from the nominal K values is obtained from Equation 2 (De Quadros *et al*., 2003; Sanusi and Amigun, 2020; Salako *et al.*, 2024).

$$K_d = \left(\frac{K - K_n}{K_n}\right) \quad (2)$$

where;
K_d represents the potassium deviation; K is the measured field potassium concentration, and K_n is the nominal potassium value.

2.4.3 F-parameter

The F-parameter proposed by Efimov (1978) is another hydrothermal indicator used in radiometric geophysical data analysis; it integrates multi-channel radiometric responses into a single enhancement metric (such as observing how observed radiometric variance departs from background expectations). The F-parameter is an important statistical measure in radiometric geophysical data analysis as it helps to identify areas with anomalous radiation levels, which can be indicative of valuable mineral deposits or other geological features. The F-parameter reflects two relevant relationships, the richness of K related to Th/U ratio and the richness of U related to the Th/K ratio, and is given by equation 3 (De Quadros *et al*., 2003; Sanusi & Amigun, 2020; Salako *et al.*, 2024).

$$.F = \frac{K \times U}{Th} = \frac{K}{\frac{Th}{U}} = \frac{U}{\frac{Th}{K}} \quad (3)$$

Where K, U, and Th are the potassium, uranium, and thorium grids, respectively.

2.4.4 Ternary map

The Ternary map used for this study integrates three key radiometric parameters: Thorium-to-Potassium ratio (Th/K), F-parameter, and potassium deviation (K_d), as these parameters can provide a composite visualization for identifying hydrothermal alteration zones associated with gold mineralization. The map delineates hydrothermal alteration zones through the combination of radiometric signatures, which are often influenced by mineralizing fluids.

2.5 Topographic Parameter Extraction

From the DEM, multiple terrain attributes were derived, including slope, aspect, curvature, and terrain ruggedness index (TRI). These parameters aid in identifying morphological expressions of faulting, folding, and lineament density patterns, which are often spatially associated with hydrothermal fluid pathways (Yakubu *et al*., 2022). Slope and curvature analyses were performed to highlight fault scarps and ridge alignments, while the ruggedness index quantified terrain complexity and potential zones of structural disruption.

3. RESULTS AND DISCUSSION

3.1 Topographic Structural Analysis

DEM-derived slope and curvature maps highlighted several geomorphological expressions of underlying geological structures. The slope (Fig. 4) and curvature maps (Fig. 5) obtained from (SRTM)-derived Digital Elevation Model (DEM) revealed distinct geomorphic expressions of fault systems and lithological contacts. These patterns observed in the slope map (Fig. 4) highlight steep gradients along major fault and fracture zones, indicating areas of intense tectonic activity. The curvature map (Fig. 5) displays alternating convex and concave topographic features, reflecting the distribution of ridges and valleys that correspond to lithological boundaries and shear zones. Areas of high curvature coincide with significant changes in slope, suggesting zones of differential erosion and possible structural weakening. Steep slope gradients and concave–convex curvature patterns are particularly concentrated along NE–SW and NW–SE trending ridges and escarpments as visible in Fig. 6. These alignments coincide with known fault traces and inferred shear zones mapped from aeromagnetic derivatives (as documented by Lawrence *et al.,* 2025), confirming their tectonic significance.

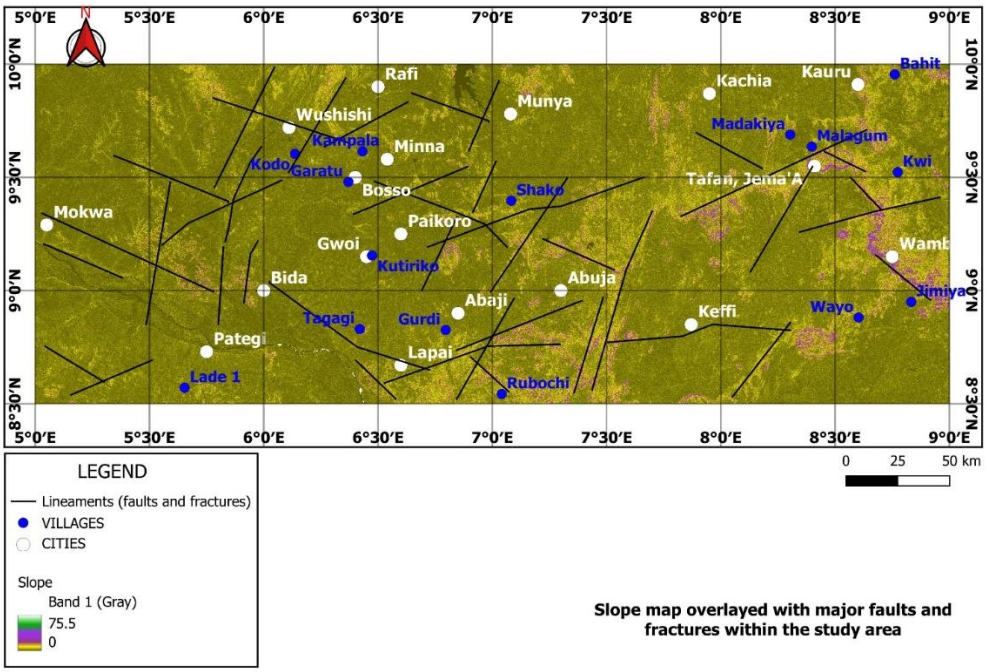

Fig. 4. Slope map derived from DEM illustrating steep gradients along major faults and fracture zones

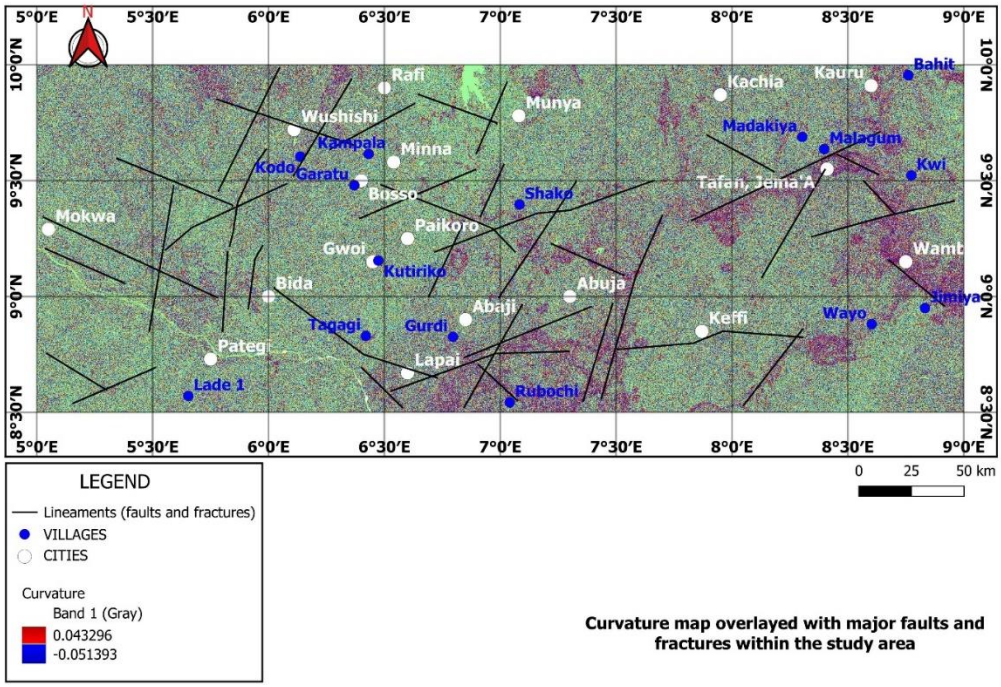

Fig. 5. Curvature map highlighting convex and concave topographic features indicative of ridges, valleys, and lithological boundaries

The structural trends and orientations as observed in the DEM contour and aspect map (Figs. 6 and 7) can serve as primary conduits for hydrothermal fluids in the region, facilitating the deposition of gold and other ore minerals. The TRI map (Fig. 8) quantifies the topographic heterogeneity of the area, revealing the roughness and complex nature of the study area

as terrain influences geological processes and patterns. High TRI (> 150) regions indicate complex regions such as ridges, while low TRI value showcases flat or smooth regions within the study area. Lineaments derived from DEM (Fig. 9a) reveal a dense network of structural features, with dominant orientations trending NE–SW and NW–SE. Areas with steep slopes are seen to coincide with convex curvature patterns and align with mapped NE–SW and NW–SE trending shear zones dominating the region, as evident in the rosette diagram (Fig. 9b).

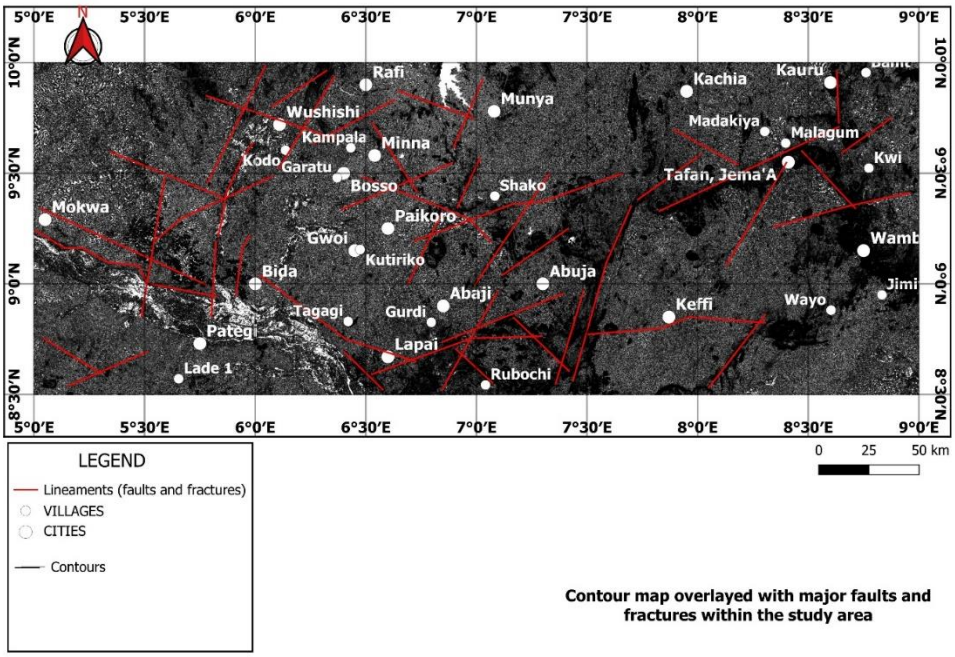

Fig. 6. Digital elevation model (DEM) contour map of the study area showing major structural trends

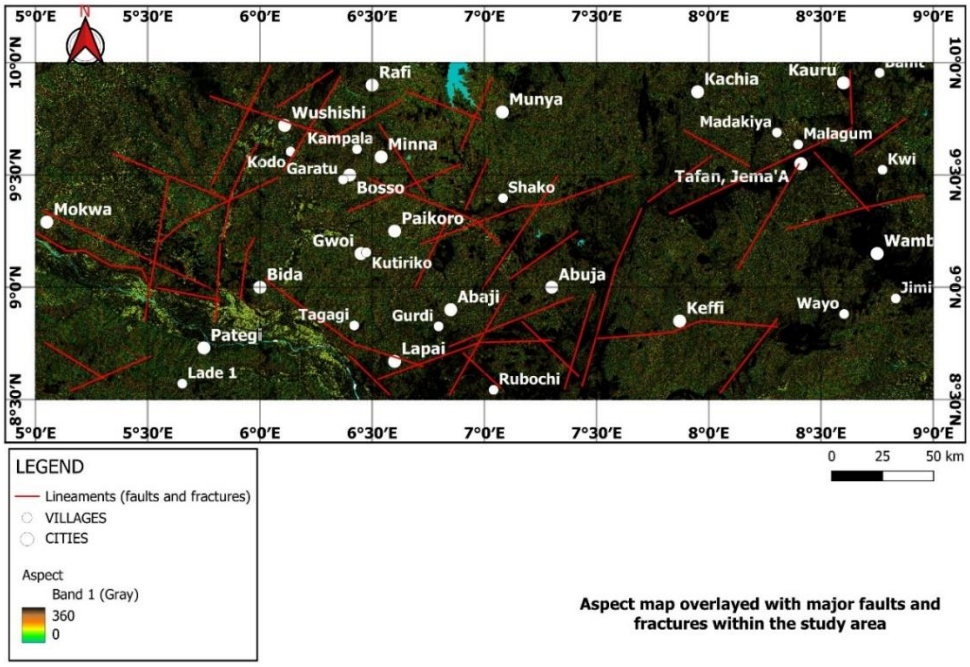

Fig. 7. Aspect map derived from DEM highlighting directions of the slope

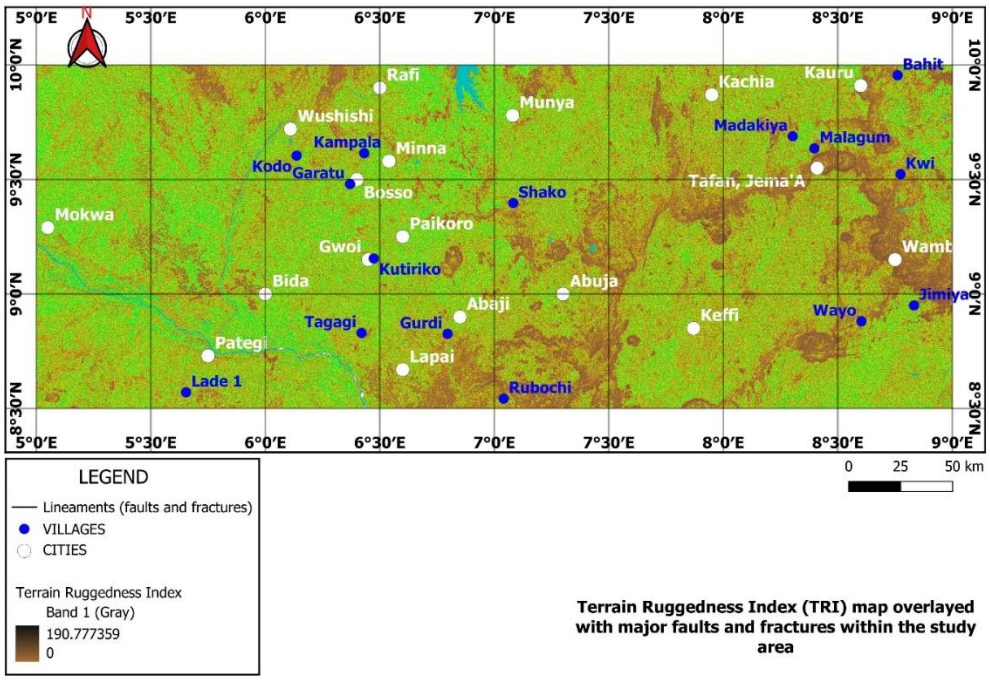

Fig. 8. Terrain ruggedness index (TRI) derived from DEM quantifying terrain complexity and potential zones of structural disruption

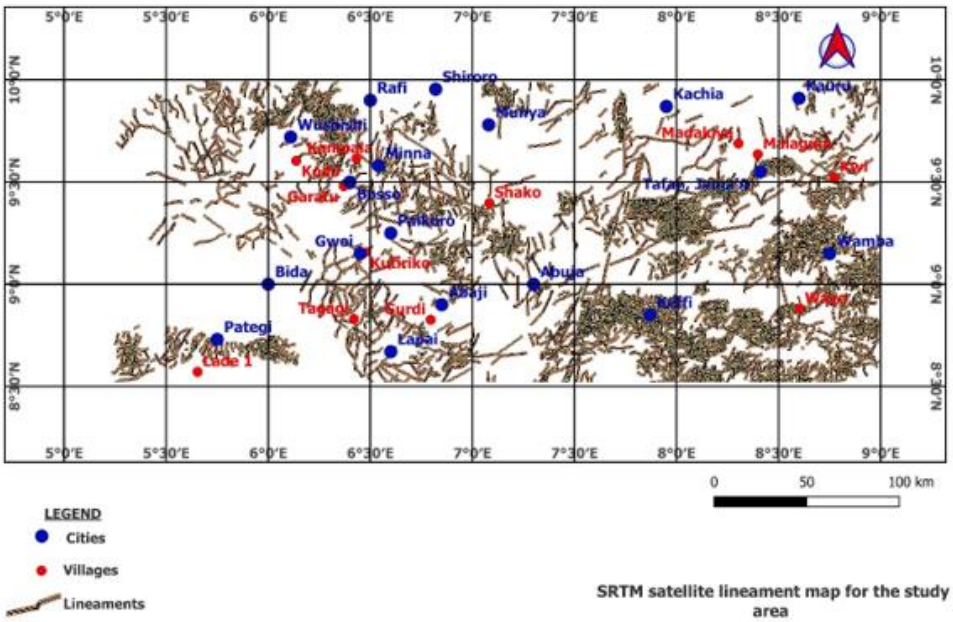

Fig. 9a. Lineament map derived from DEM showing dominant NE–SW, NW–SE, and E-W trends

The SRTM-DEM lineament rosette diagram (Fig. 9b) displays the directional distribution of the SRTM-DEM extracted linear features representing lineament frequency across azimuth classes in 10° intervals. The bars indicate the dominant structural orientations, with the red and orange bars representing the most frequent orientations. The highest concentration of lineaments falls along the 3°–8°,120°–130°, and 90°–100°azimuth, suggesting the presence of dominant NE–SW, NW-SE, and E-W structural trends in the area. This direction is reflected by the longest and most saturated red and orange bars on the rosette. These trends are in

agreement with results obtained from research carried out in Nigeria by Abraham *et al.* (2024), Egbelehulu and Abu (2024), Arogundade *et al.* (2022), and that carried out in Cameroon by Anaba Fotze *et al.* (2024), affirming the Pan-African structural trend. These trends are seen to coincide with those showcased in the gold occurrence zone map (Fig. 10).

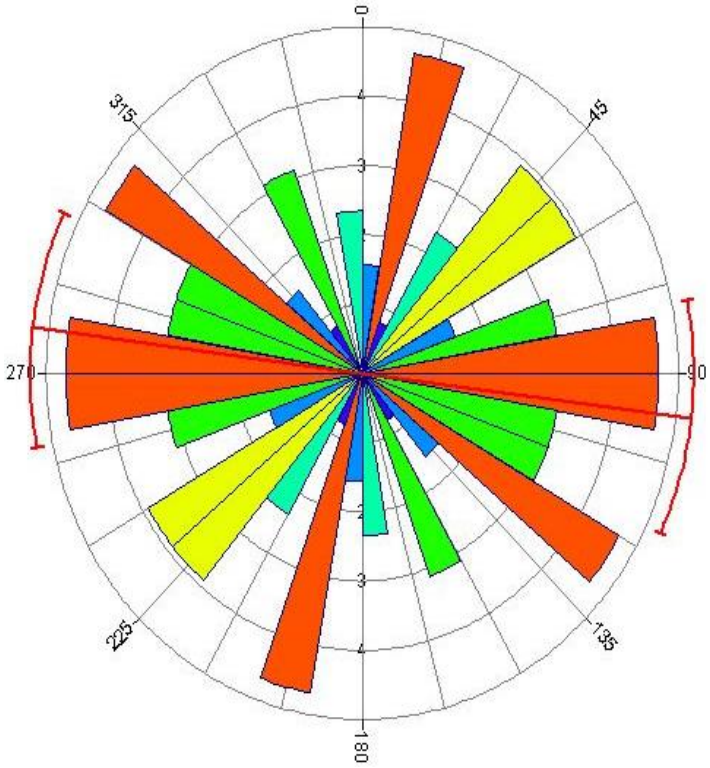

SRTM Statistical Summary	
Calculation Method:	Frequency
Class Interval:	10.0 Degrees
Min.Length Filtering:	Deactivated
Max.Length Filtering:	Deactivated
Azimuth Filtering:	Deactivated
Data Type:	Bidirectional
Population:	64
Total Length of All Lineations:	6,164,152.69
Maximum Bin Population:	6.0
Mean Bin Population:	3.76
Standard Deviation of Bin Population:	1.72
Maximum Bin Population (%):	4.69
Mean Bin Population (%):	2.94
Standard Deviation of Bin Population (%):	1.35
Maximum Bin Length:	547,888.28
Mean Bin Length:	181,298.61
Standard Deviation of Bin Lengths:	163,826.02
Maximum Bin Length (%):	8.89
Mean Bin Length (%):	2.94
Standard Deviation of Bin Lengths (%):	2.66
Vector Mean:	97.2 Degrees
	277.21 Degrees
Confidence Interval:	18.9 Degrees
	(95 Percent)
R-mag:	0.49

Fig. 9b. Rossette diagram derived from DEM showing dominant NE–SW, NW–SE, and E-W trends

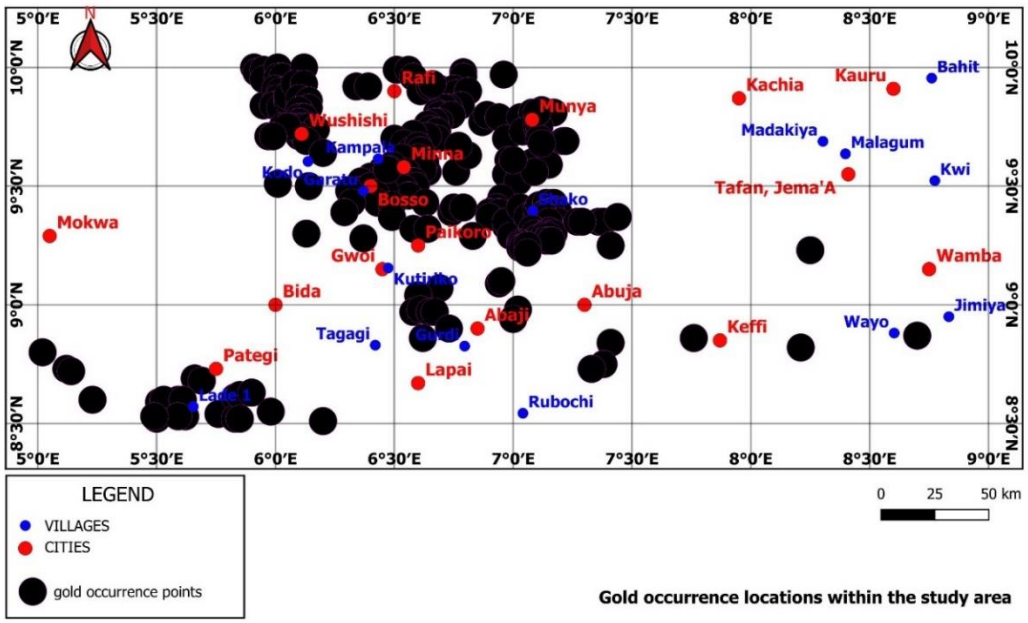

Fig. 10. Gold occurrence locations within the study area extracted from the mineral resources map of Nigeria (Source: NGSA, 2023b)

3.2 Radiometric Alteration Mapping

The processed radiometric datasets revealed distinct spatial variations across the study area, corroborating the structural observations from the DEM data analysis. The Total count (TC) map (Fig. 11) reflects the cumulative gamma emissions from the decay of naturally occurring radioactive elements, primarily potassium (K), Thorium (Th), and Uranium (U) in rocks and soils within the study region, expressed in counts per second (cps), which are sensitive indicators of lithological variation and hydrothermal alteration. The values range from approximately 6.206 to 35.639 cps, with low counts depicted in blue and green shades, and high counts represented by yellow, orange, red, and pink colours. Elevated total gamma count values are associated with felsic lithologies, intrusive bodies, or hydrothermally altered zones enriched in potassium-bearing minerals such as sericite, biotite, and K-feldspar. These minerals are common products of potassic alteration, which is often spatially and genetically related to gold mineralization in orogenic and intrusion-related systems.

The high gamma anomalies (orange to pink zones: >23 cps) observed in the central and eastern parts of the study area, particularly around Wamba, Kachia, and parts of Paikoro and Wushishi, are interpreted as potential hydrothermal alteration zones coinciding with migmatitic gneiss, granite gneiss, porphyritic granite, granite and granite porphery, and undifferentiated schist geologic units within the study area. These regions are likely areas of hydrothermal alteration or pegmatitic intrusions that have undergone potassium enrichment through fluid-rock interaction, as also visible in the potassium concentration map (Fig. 12), making them significant targets for further gold prospectivity investigation. These anomalies align with regions where artisanal gold mining activities have been recorded around Wuna, Chechey, and Pangu, as documented by Ayuba and Abu (2024) and around Paiko and Minna, as shown in Fig. 2, suggesting a genetic relationship between potassic alteration and mineralization.

Conversely, areas with low total count values (blue to green zones: <13 cps) correspond to mafic, fresh basalts or less altered basement rocks, which are generally less favourable for gold mineralization. However, these zones may still play a structural or lithological role as footwalls or barriers controlling fluid pathways in the region.

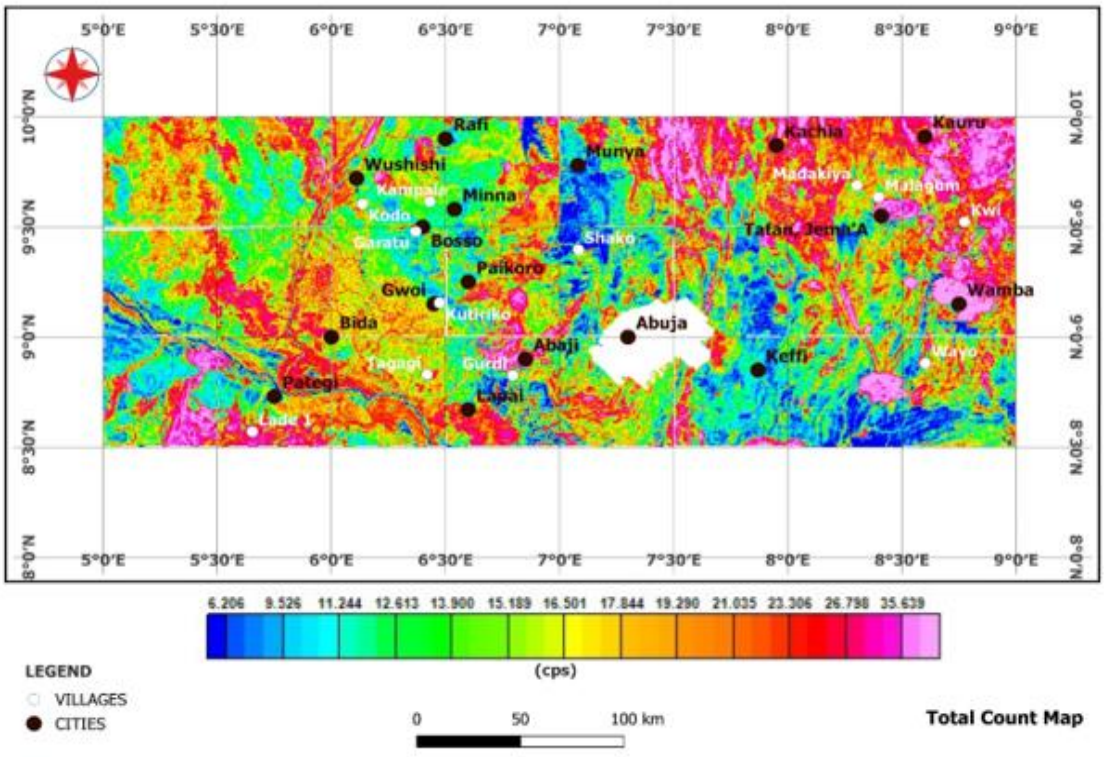

Fig. 11. The total count map of the study area

In the K/Th map (Fig. 13), the values range from –0.039 to 0.346 %/ppm, with low ratios (shown in blue and green shades) reflecting relatively unaltered or thorium-rich zones. Higher ratios (depicted in yellow, red, and pink colours) suggest potassium-enriched alteration zones**.** The highest K/Th anomalies, also indicating argillic alteration, represented in pink (values > 0.205 %/ppm), are observed primarily in the southeastern and northeastern parts of the study area, including regions around Wamba, Wayo, Keffi, Kachia, Wushishi, Minna, Abaji, and Munya**.** These zones are interpreted as potential hydrothermal alteration fronts**,** possibly linked to gold mineralization, given their radiometric signature and alignment with regional structures. Moderate K/Th anomalies are also visible around Madakiya and Malagum, coinciding with a younger basalt geologic unit, which may suggest transitional alteration halos. In contrast, low-ratio zones in blue to cyan are notable around Bida and Lapai (Nupe sandstone geologic unit), and at the southeast edge of the study area **(**Meta-conglomerate**)**. These indicate areas dominated by resistant thorium-bearing minerals, which are less likely to host gold-bearing alteration zones.

In Fig. 14, the Thorium-to-Potassium (Th/K) ratio map (the inverse of the K/Th map), different colour ranges represent varying Th/K ratios. High values (depicted in pink, purple, and red hues) around Bida, Tagagi, and western Pategi, indicate low K concentration, hence an argillic alteration. These zones may indicate the presence of mineralizing fluids or past hydrothermal activity. Regions with low Th/K ratios, observed around Wamba (with a biotite granite geologic unit), and parts of the central and southeastern sectors, indicate sericitic or argillic alteration. These low Th/K ratios zones (outlined with white dashed lines) are structurally complex areas and correlate with high K/Th (Fig. 13), associated with potassic alteration commonly linked to gold mines, as visible in Fig. 2. Hence, key targets for further exploration.

The F-parameter map (Fig. 15) further refined the identification of alteration zones by combining potassium and thorium signals, delineating areas with strong geochemical contrasts. Studies in the Igarra Schist Belt (Ohwo & Fadeyi, 2024) have used the F-parameter on airborne radiometric data to enhance the detection of alteration zones in structurally complex areas**.** The F-parameter map, computed as a function of the concentrations of potassium (K), thorium (Th), and uranium (U), serves as a diagnostic indicator of hydrothermal alteration, particularly in terrains affected by potassic enrichment or metasomatic processes associated with gold mineralization.

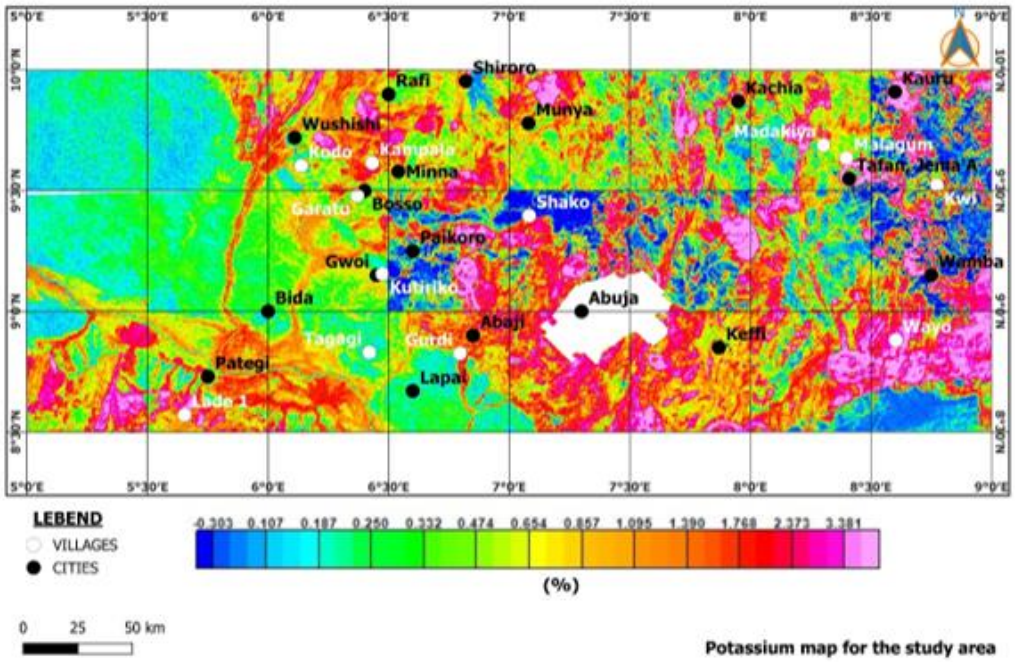

Fig. 12. Potassium (K) concentration map showing potassium enrichment around granitic intrusions and altered rock units

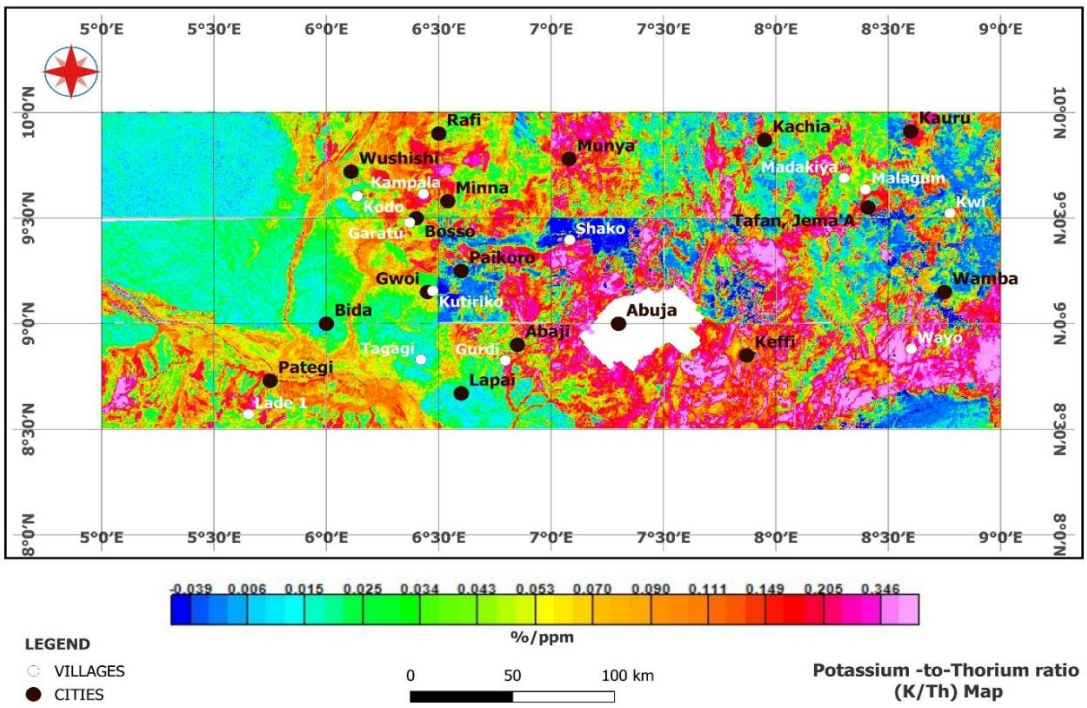

Fig. 13. The Potassium-to Thorium ratio (K/Th) map of the study area

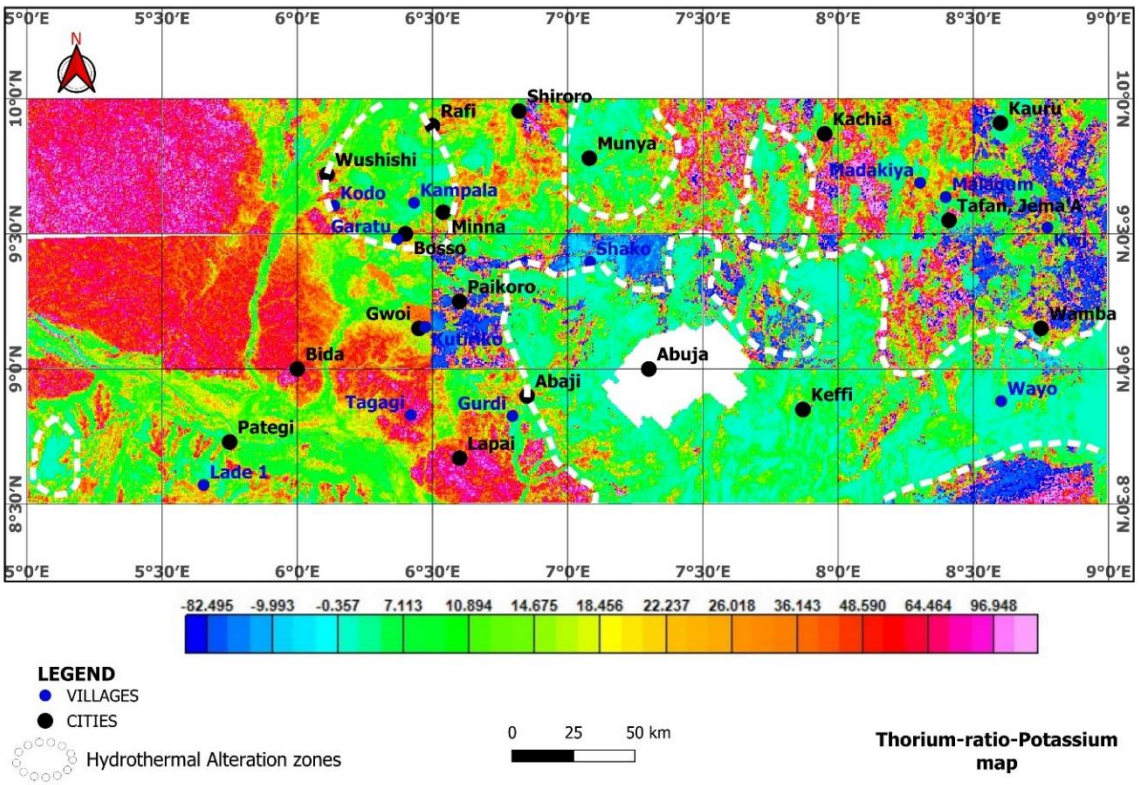

Fig. 14. Th/K ratio map identifying hydrothermally altered zones (outlined with white dashed boundaries) along shear and fracture systems

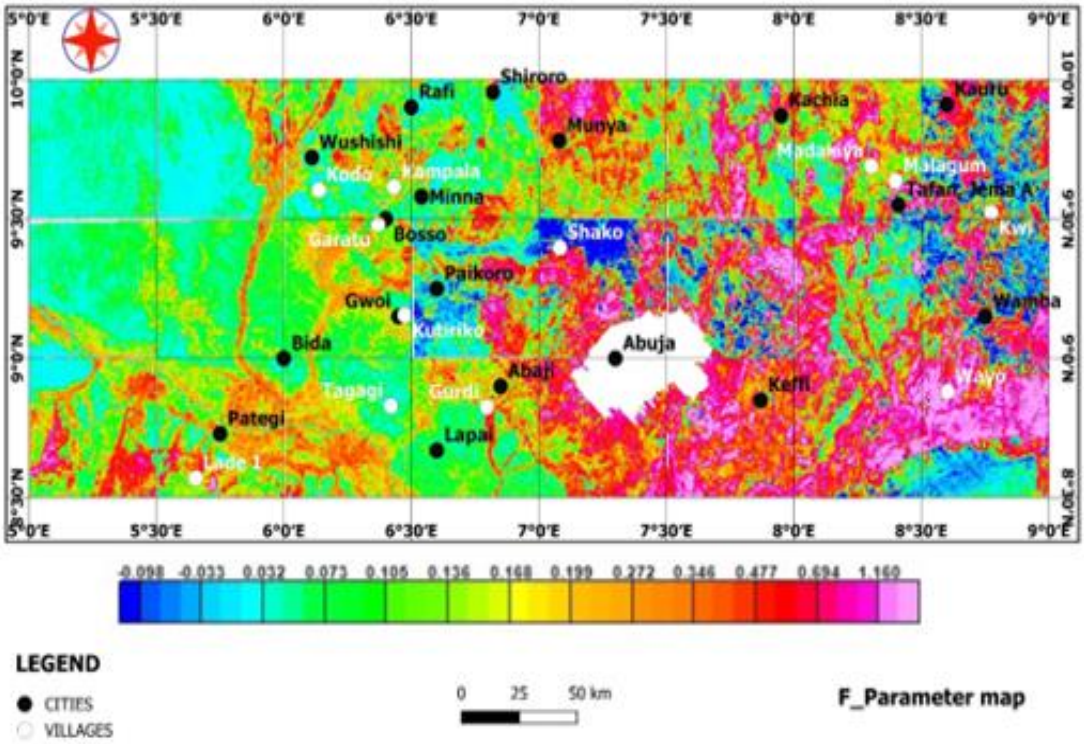

Fig. 15. The F-parameter map integrating multi-channel radiometric data (K, Th, and U) exhibits pronounced high-intensity zones in the central, northeastern, and southeastern portions of the study area

The mapped values range from –0.098 to 1.160, with the colour spectrum extending from blue (low values) through green and yellow to red and pink (high values). Regions characterized by high F-parameter values (greater than 0.3), indicated by orange to pink hues, are interpreted as zones of enhanced radioelement concentration, especially potassium, which is typically mobilized and concentrated in potassic, sericitic, argillic, and propylitic alteration zones. This alteration is a product of hydrothermal fluid activity, and it plays a critical role in the emplacement of gold-bearing minerals.

Notably, high F-parameter regions, with undifferentiated schist, biotite granite, migmatite, and granite gneiss rock units, are concentrated in the eastern and southeastern parts of the study area, particularly around Munya, Wamba, Kachia, and Wayo. These zones are therefore considered highly prospective for gold mineralization. In contrast, areas with low F-parameter values (less than 0.1), shown in blue and green colours, dominate the western portion of the study area, including locations such as Pategi, Tagagi, and Bida, made up of sandstone and siltstone (Nupe sanstone). These low-intensity zones are indicative of relatively unaltered or weakly altered basement rocks with limited hydrothermal overprint, and are therefore considered less prospective for gold mineralization.

The K-deviation map (Fig. 16) represents the spatial variability of potassium concentration anomalies across the study area. Recent studies in parts of Kebbi state (Salako *et al*. 2024) have shown the effectiveness of K_d in identifying varying alteration zones associated with gold mineral deposits. K-deviation specifically highlights how much potassium concentration at each point deviates from the regional background average, and areas of high deviation typically indicate zones of potassic enrichment, often linked to hydrothermal alteration processes that are commonly associated with gold mineralization.

The colour gradient on the map ranges from deep blue (indicating the lowest deviation values around 1.519) through green and yellow (representing moderate deviations), to bright red and pink (showing the highest deviation values up to 3.595). Zones with high K-deviation,

particularly those marked in pink, red, and orange, suggest significant potassic alteration (Eleraki *et al.,* 2017; Ohwo & Fadeyi, 2024) and may reflect areas where hydrothermal processes have affected the bedrock. These include notable locations such as Wushishi, Kampala, Minna, Abaji, Gurdi, Wayo, Shako, Munya, and Keffi, which stand out as areas with potentially favourable conditions for gold mineralization. Compared with geology, these high K_d regions coincide with the presence of migmatitic gneiss, granite gneiss, porphyritic granite, granite and granite porphery, and undifferentiated schist. Conversely, low-deviation zones shown in blue to green, like those around Kutiriko, Bida, Lapai, and Gwoi, coinciding with Nupe sandstone (felcspathic sandstone and siltstone), may indicate limited alteration or background geochemical conditions less favourable for gold deposition.

The potassium ternary map (Fig. 17) combines the concentration of Potassium (K), the K/Th (Potassium-to-Thorium) ratio, and the K/U (Potassium-to-Uranium) ratio to highlight hydrothermal alteration zones across the study area, which are potentially favourable for gold mineralization. The colour composite in the ternary triangle showcases three colours: red colour, which signifies areas rich in potassium, green regions with elevated K/Th ratios (indicating potassium enrichment possibly due to hydrothermal activity), and the blue regions, which reflect high K/U ratios (suggestive of potassium mobilization relative to uranium).

In the map (Fig. 17), hydrothermal alteration zones are represented by dashed white polygons and are distributed across multiple locations, including Paikoro, Lapai, Wushishi, Rafi, Munya, Madakiya, Wamba, and Keffi. These zones show a distinct geochemical footprint associated with potassic alteration, which is often linked to gold mineralizing systems, especially in structurally controlled environments such as shears and faults. The map integrates the behaviour of radioactive elements influenced by alteration processes. Areas with strong red, green, and blue colorations suggest hydrothermal enrichment of potassium or depletion of thorium and uranium due to leaching or fluid interaction. These processes are characteristic of hydrothermal systems, which commonly transport and deposit gold.

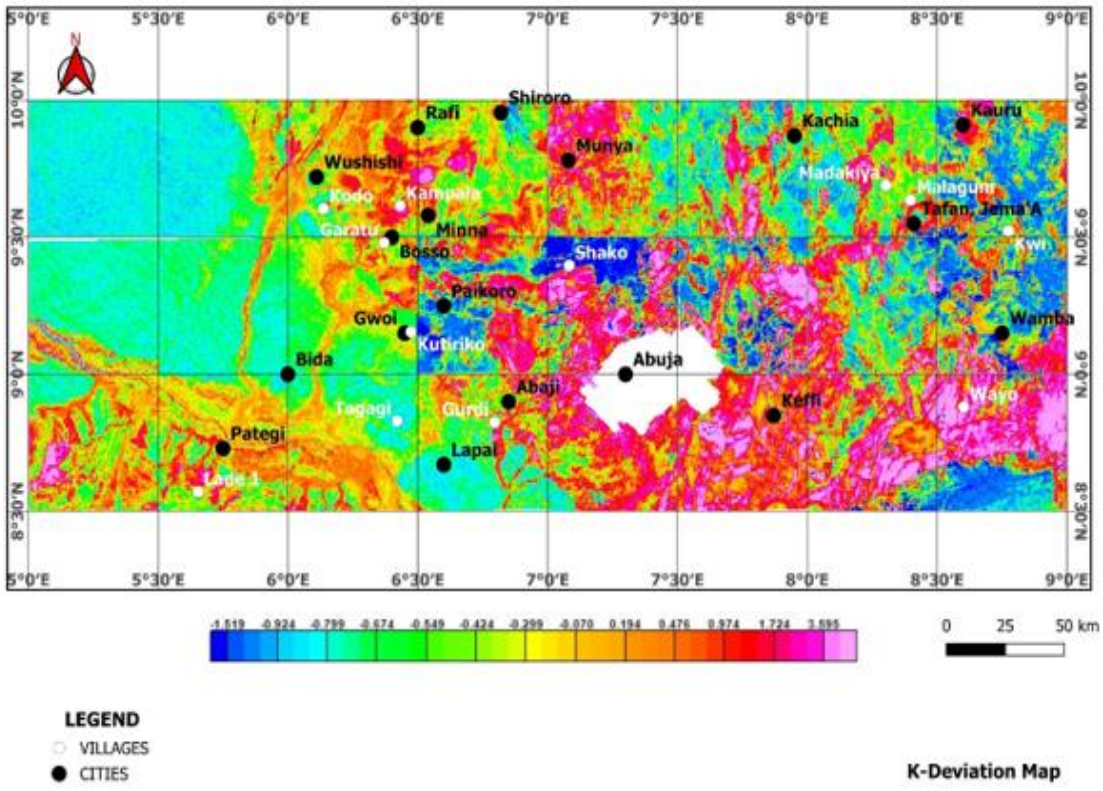

Fig. 16. K-deviation map representing the spatial variability of potassium concentration across the study area

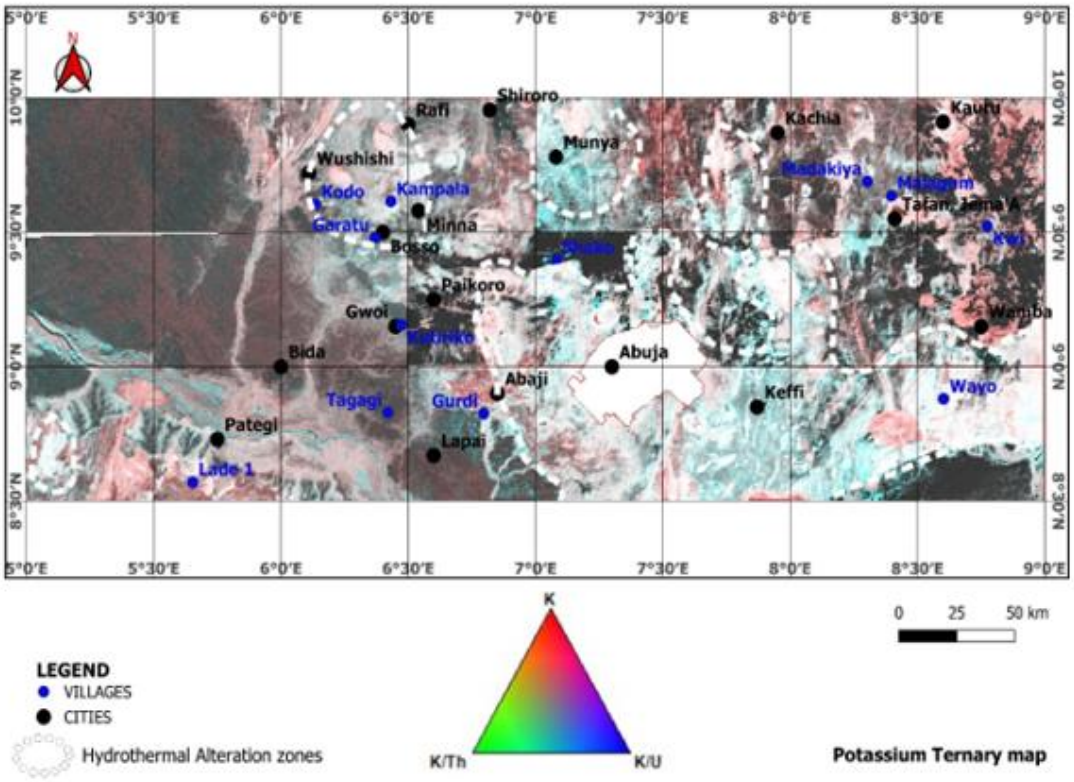

Fig. 17. The Potassium Ternary map, which combines the concentration of Potassium (K), the K/Th (Potassium-to-Thorium) ratio, and the K/U (Potassium-to-Uranium) ratio to highlight hydrothermal alteration zones across the study area

The hydrothermal ternary map (Fig. 18) integrates three key radiometric parameters, the Thorium-to-Potassium ratio (Th/K), the F-parameter, and Potassium deviation (K_d), and provides a composite visualization for identifying hydrothermal alteration zones associated with gold mineralization, as was used by Salako *et al.* (2024) in the delineation of hydrothermal alteration zones in the Zuru-Yauri schist belt of Kebbi state. The map delineates hydrothermal alteration zones through the combination of radiometric signatures, which are often influenced by mineralizing fluids. In the map, different colours represent varying combinations of the three parameters. Red areas indicate high Th/K ratios, which may reflect thorium enrichment or potassium depletion due to alteration. Green areas correspond to high F-parameter values, which are sensitive indicators of compositional changes typically caused by hydrothermal processes. Blue regions represent high potassium deviation (K_d), which may suggest zones of potassic alteration, a known feature in many gold-bearing systems. The hydrothermal alteration zones, black dashed outlines, highlight specific regions where the three indicators converge, suggesting significant alteration. These areas include parts of Munya, Wushishi, Paikoro, Kutiriko, Kauru, and Shako, among others. These zones coincide with previously identified structural trends and geological units such as migmatite, migmatitic gneiss, granite gneiss, porphyritic granite, granite and granite porphery, biotite granite, and undifferentiated schist favourable for gold mineralization.

3.3 Integrated Structural–Radiometric Output

The normalized and weighted integration of radiometric and topographic datasets produced a composite structural–alteration map superimposed on the geology map for the study area (Fig. 19). The integration highlighted several high-priority target zones, predominantly clustered in the central and northeastern parts of the study area, as documented by Lawrence *et al.* (2025). Comparison with known artisanal mining sites around Minna, Paiko, and those captured by Ayuba and Abu 2024 at the Abaji axis (Wuna, Chechey, and Pangu district) as

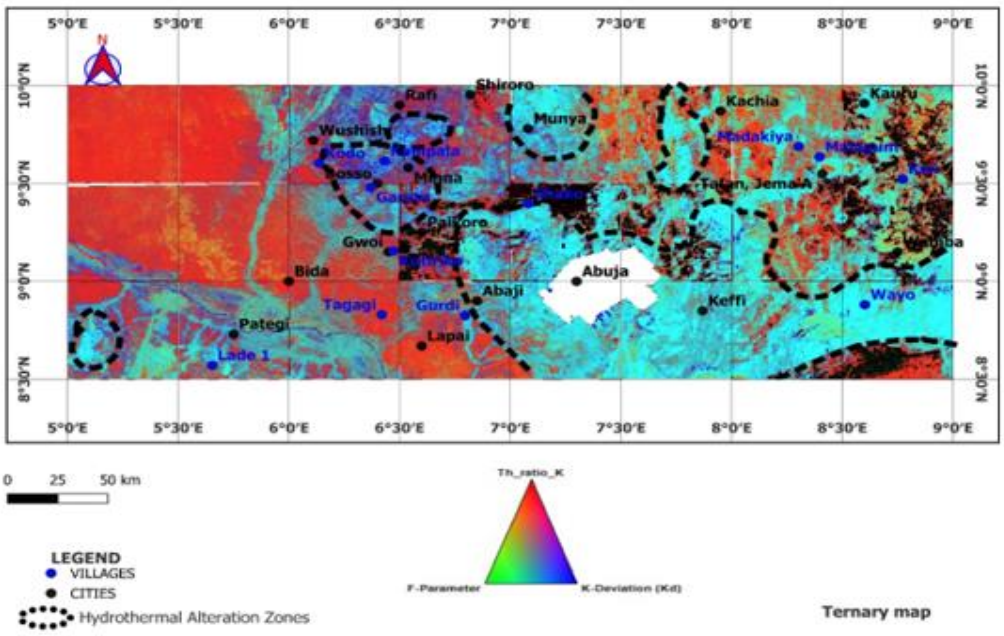

Fig. 18. The hydrothermal ternary map for the study area which integrates three key radiometric parameters, Thorium-to-Potassium ratio (Th/K), F-parameter, and Potassium deviation (K_d), and provides a composite visualization for identifying hydrothermal alteration zones (outlined with black dash lines)

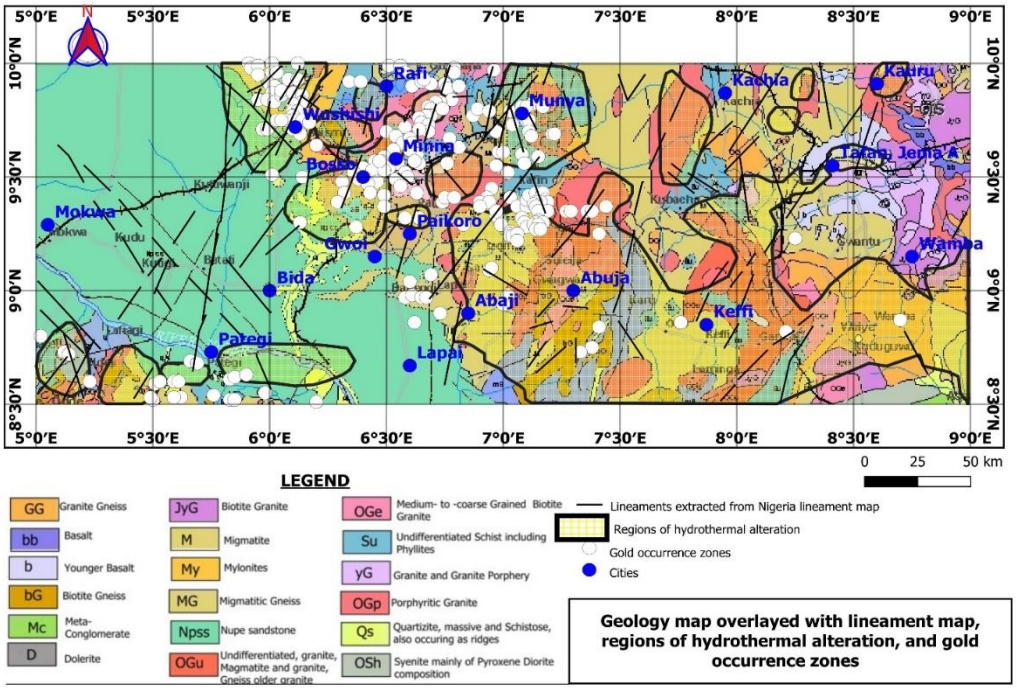

Fig. 19. Geology map overlayed with lineaments, zones of hydrothermal alteration, and gold occurrence zones

shown in Fig. 2, more than 70% of these sites fall within or near high-potential zones identified in the integrated map (Fig. 19). These high-potential zones are characterized by the convergence of high lineament density (Fig. 9a), high slope gradients, as shown in Fig. 4, convex

curvature observed in Fig. 5, elevated K/Th ratios seen in Fig. 12, and significant F-parameter anomalies (Fig. 15). Hence, the areas with high lineament density correspond to zones of elevated radiometric anomalies and steep slopes. These areas are seen to align well with known gold occurrence locations showcased in Fig. 19, and hence, are interpreted as structurally prepared and geochemically favourable sites for hydrothermal alteration and possible gold mineralization, validating the effectiveness of the integrated approach.

The NE–SW trends, prominent in the region, align with regional tectonic fabrics and are commonly associated with gold-bearing quartz veins in similar geological settings. The results align with recent global trends emphasizing the effectiveness of multi-criteria integration in mineral exploration as carried out by Abubakar (2023), where topographic, structural, and radiometric proxies are merged to improve target definition accuracy.

4. CONCLUSION

This study demonstrates the effectiveness of integrating topographic and radiometric datasets for enhancing structural mapping in gold exploration within the basement terrain of North-Central Nigeria. Through the analysis of Shuttle Radar Topography Mission (SRTM) derivatives such as slope and curvature, coupled with radiometric data including potassium, thorium, and uranium distributions, the research successfully delineated key structural features and hydrothermal alteration zones. The combined use of lineament mapping, density analysis, and radiometric ratios (K/Th and F-parameter) highlighted zones of structural complexity, which are strongly correlated with known gold occurrences in the study area.

The results revealed that the dominant NE-SW, NW-SE, and E-W lineament orientations, as showcased in Fig. 9b, are not only consistent with the regional tectonic framework of the Nigerian basement complex but also play a crucial role in localizing gold mineralization. These orientations correspond with shear zones and fracture systems that act as conduits for hydrothermal fluids, thereby controlling the emplacement of mineral deposits. The radiometric anomalies further emphasized areas of potassic enrichment and hydrothermal alteration, validating their association with gold-bearing zones. By combining topographic and radiometric data, this study provides a cost-effective and efficient approach to identifying priority exploration targets. The findings confirm that integrated geospatial analysis significantly improves the accuracy of structural interpretations, reduces exploration risks, and guides follow-up geophysical and geochemical surveys.

DISCLAIMER (ARTIFICIAL INTELLIGENCE)

Authors hereby declare that NO generative AI technologies such as Large Language Models (ChatGPT, COPILOT, etc) and text-to-image generators have been used during writing or editing of this manuscript.

COMPETING INTERESTS

Authors have declared that they have no known competing financial interests or non-financial interests, or personal relationships that could have appeared to influence the work reported in this paper.

REFERENCES

Abdelrady, M., Moniem, M. A., Alarfi, S. S., Abdelrady, A., Othman, A., Mohammed, M. A. A., & Mohamed, A. (2023). Geophysical investigation for the identification of subsurface features influencing mineralization zones. *Journal of King Saud University-Science, 35*(7). https://doi.org/10.1016/j.jksus.2023.102809

Abraham, E. M., Uwaezuoke, A. E., & Usman, A. O. (2024). Geophysical investigation of subsurface mineral potentials in North-Central Nigeria: Implications for sustainable mining and development. *Geomechanics and Geophysics for Geo-Energy and Geo-Resources, 10*, 192. https://doi.org/10.1007/s40948-024-00913-3

Abubakar, F. (2023). Investigation of iron ore potential in north-central Nigeria, using high-resolution aeromagnetic dataset and remote sensing approach. *Heliyon, 10*(1), e23618. https://doi.org/10.1016/j.heliyon.2023.e23618

Ahmed, A. L., Abubakar, W. M., & Abubakar, A. (2021). Measurement of radioelements (U, Th and K) concentration using ground radiometric and statistical studies at Gaya North-Western Nigeria. *International Journal of Research and Scientific Innovation (IJRSI), VIII*(IX). ISSN 2321-2705

Ajibade, P. A., & Kolawole, G. A. (2008). Synthesis, characterization and in vitro antiprotozoal studies of iron (III) complexes of some antimalarial drugs. *Journal of Coordination Chemistry*, *61*(21), 3367-3374.

Akinlalu, A. A. (2023). Radiometric mapping for the identification of hydrothermally altered zones related to gold mineralization in the Ife–Ilesa Schist Belt, Southwestern Nigeria. *Indonesian Journal of Earth Sciences / Indonesian Journal of Earth Sciences Knowledge & Applications, 6*(3), 153–164. https://doi.org/10.52562/injoes.2023.519

Akinluyi, F. O., Olorunfemi, M. O., & Bayowa, O. (2021). Application of remote sensing, GIS and geophysical techniques for groundwater potential development in the crystalline basement complex of Ondo State, Southwestern Nigeria. *Sustainable Water Resources Management, 7*(4), 1–15. https://doi.org/10.1007/s40899-020-00486-5

Akintola, O. F., & Adekeye, J. I. D. (2008). Mineralization potentials of pegmatites in the Nasarawa area of Central Nigeria. *Earth Sciences Research Journal, 12*(2), 213–234.

Anaba Fotze, Q. M., Bi-Alou, M. B., Ndougsa-Mbarga, T., Bailly, L., Bernard, J., Penaye, J., Sep Nlomngan, J. P., Djieto Lordon, A. E., Ketchaya, Y. B., & Moussango Ibohn, P. A. (2022). Integrating ASTER 07XT, Landsat 8, and aeromagnetic data for the delineation of potential mineralization sites in North Cameroon. *Geological Journal, 57*(9), 3949–3971. https://doi.org/10.1002/gj.4513

Anaba Fotze, Q. M., Palai, F., Bi-Alou, M. B., Lordon, A. E. D., Ndougsa-Mbarga, T., Neh Fru, M. M., Lyonga, D. I., & Rodo, G. N. (2024). Aeromagnetic and field data characterization of structural features for the delineation of potential gold mining sites in Northern Cameroon: A case study of Tchollire and environs. *Acta Geophysica, 72*, 1637–1659. https://doi.org/10.1007/s11600-023-01166-6

Andongma, W. T., Gajere, J. N., Amuda, A. K., Edmond, R. R. D., Faisal, M., & Yusuf, Y. D. (2021). Mapping of hydrothermal alterations related to gold mineralization within parts of the Malumfashi Schist Belt, North Western Nigeria. *The Egyptian Journal of Remote Sensing and Space Science, 24*(3), 401–417. https://doi.org/10.1016/j.ejrs.2020.11.001

Arogundade, A. B., Awoyemi, M. O., Hammed, O. S., Falade, S. C., & Ajama, O. D. (2022). Structural investigation of Zungeru-Kalangai fault zone, Nigeria using aeromagnetic and remote sensing data. *Heliyon, 8*(3), e09055. https://doi.org/10.1016/j.heliyon.2022.e09055

Ayoola, Y. J., Olusola, J. O., & Samuel, O. A. (2019). Organic petrography, Rock–Eval pyrolysis and biomarker geochemistry of Maastrichtian Gombe Formation, Gongola Basin, Nigeria. *Journal of Petroleum Exploration and Production Technology.* https://doi.org/10.1007/s13202-019-00770-x

Ayuba Bwamba Jonah, & Abu Mallam. (2024). Integrated interpretation of aeromagnetic and aero-radiometric data to delineate structures and hydrothermal alteration zones associated with gold mineralization in parts of North-Central Nigeria. *Asian Journal of Geological Research (AJOGER), 7*(2), 136–153. https://journalajoger.com/index.php/AJOGER/article/view/161

Baratoux, D., Fall, M., Meslin, P.-Y., Jessell, M. W., Vanderhaeghe, O., Moyen, J. F., Ndiaye, P. M., Boamah, K., Baratoux, L., & André-Mayer, A. S. (2021). The impact of measurement scale on the univariate statistics of K, Th, and U in the Earth crust. *Earth and Space Science, 8*, e2021EA001786. https://doi.org/10.1029/2021EA001786

Chinwuko, A., Usman, A., Onwuemesi, A., Anakwuba, E., Okonkwo, C., & Bemsen, I. (2014). Interpretations of aeromagnetic data over Lokoja and environs, Nigeria. *International Journal of Advanced Geosciences, 2*. https://doi.org/10.14419/ijag.v2i2.2305

Chiozzi, P., Pasquale, V., & Verdoya, M. (2007). Radiometric survey for exploration of hydrothermal alteration in a volcanic area. *Journal of Geochemical Exploration, 93*(1), 13–20. https://doi.org/10.1016/j.gexplo.2006.07.002

De Quadros, T. F., Koppe, J. C., Strieder, A. J., & Costa, J. F. C. (2003). Gamma-ray data processing and integration for lode-Au deposits exploration. *Natural Resources Research, 12*, 57–65.

Ebele, J. E., Ofoegbu, C. O., & Nur, A. (2021). Interpretation of high-resolution aeromagnetic and radiometric data for delineation of mineral potential zones over Abuja and environs, North-Central Nigeria. *Arabian Journal of Geosciences, 14*, 1947. https://doi.org/10.1007/s12517-021-07915-5

Efimov, A. V. (1978). Multiplikativnyj pokazatel dlja vydelenija endogennych rud poaerogamma-spektrometriceskim dannym. *Metody Rudnoj Geofiziki*, *Leningrad, Naucno-Proizvodstvennoje Objedinenie Geofizika, 163*, 59–68.

Egbelehulu, P., & Abu, M. (2024). Integration of ground magnetic method and whole-rock analysis for solid mineral prospecting in a part of Abuja, Nigeria. *Pakistan Journal of Geology (PJG), 8*(1), 67–73. http://doi.org/10.26480/pjg.01.2024.67.73

Ekwok, S. E., George, A. M., Omori, A. A., Abdelrahman, K., Ugar, S. I., Andráš, P., Morphy, M. I., Akpan, A. E., & Eldosouky, A. M. (2024). Unveiling the mineral resources and structural patterns in the Middle Benue Trough: A comprehensive exploration using airborne magnetic and radiometric data. *Geocarto International, 39*(1). https://doi.org/10.1080/10106049.2024.2339290

Eldosouky, A. M., Eleraki, M., Mansour, A., Saada, S. A., & Zamzam, S. (2024). Geological controls of mineralization occurrences in the Egyptian Eastern Desert using advanced integration of remote sensing and magnetic data. *Scientific Reports, 14*(1), Article 16700. https://doi.org/10.1038/s41598-024-66924-y

Eleraki, M., Ghieth, B., Abd-El Rahman, N., & Zamzam, S. (2017). Hydrothermal zones detection using airborne magnetic and gamma ray spectrometric data of mafic/ultramafic rocks at Gabal El-Rubshi area, Central Eastern Desert (CED), Egypt. *Advances in Natural and Applied Sciences, 11*(9), 182–196.

Frutuoso, R., Lima, A., & Teodoro, A. C. (2021). Application of remote sensing data in gold exploration: Targeting hydrothermal alteration using Landsat 8 imagery in northern Portugal. *Arabian Journal of Geosciences, 14*(6), 459. https://link.springer.com/article/10.1007/s12517-021-06786-0

Hamimi, Z., & Abd El-Wahed, M. A. (2019). Suture (s) and major shear zones in the Neoproterozoic basement of Egypt. *The Geology of Egypt*, 153-189.

Hronsky, J. M. A., & Groves, D. I. (2008). Science of targeting: Definition, strategies, targeting and performance measurement. *Australian Journal of Earth Sciences, 55*(1), 3–12.

International Atomic Energy Agency (IAEA). (2003). *Guidelines for radioelement mapping using gamma ray spectrometry data (IAEA-TECDOC-1363)*. IAEA, Vienna.

Lawrence, J. O., Abu, M., Nasir, N. A., & Gajere, J. N. (2025). Integrated gravity and magnetic derivative modelling for structural control of gold mineralization in North-Central Nigeria. *Asian Journal of Geological Research, 8*(3), 376–391. https://doi.org/10.9734/ajoger/2025/v8i3205

Lukman, L. M., Najime, T., Ogunleye, P. O., Magaji, S., & Caleb, N. K. (2024). Geology and geochemical characterization of basement rocks around Burumburum Area, North Central Basement Complex, Nigeria. *Earth Sciences, 13*(1), 14–38. https://doi.org/10.11648/j.earth.20241301.13

Mamouch, Y., Attou, A., Miftah, A., Ouchchen, M., Dadi, B., Achkouch, L., Et-tayea, Y., Allaoui, A., Boualoul, M., Randazzo, G., Lanza, S., & Muzirafuti, A. (2022). Mapping of hydrothermal alteration zones in the Kelâat M'Gouna region using airborne gamma-ray spectrometry and remote sensing data: Mining implications (Eastern Anti-Atlas, Morocco). *Applied Sciences, 12*(3), 957. https://doi.org/10.3390/app12030957

Nigeria Geological Survey Agency (NGSA). (2023a). *Geological maps*. https://ngsa.gov.ng/geological-maps/

Nigeria Geological Survey Agency (NGSA). (2023b). *Geological maps – Mineralization map of Nigeria*. https://ngsa.gov.ng/geological-maps/

Obaje, N. G. (2009). *Geology and mineral resources of Nigeria*. Springer. https://doi.org/10.1007/978-3-540-92685-6

Ogunmola, J. K., Gajere, E. N., Ayolabi, E. A., Olobaniyi, S. B., Jeb, D. N., & Agene, I. J. (2015). Structural study of Wamba and environs, North-Central Nigeria using aeromagnetic data and NigeriaSat-X image. *Journal of African Earth Sciences, 111*(1), 307–321.

https://doi.org/10.1016/j.jafrearsci.2015.07.028

Ohwo, M. U., & Fadeyi, S. S. (2024). Integration of ASTER and airborne radiometric data in the exploration for hydrothermal alteration zones associated with mineral deposits in Igarra Schist Belt, Nigeria. *International Journal of Earth Sciences Knowledge & Applications, 6*(2), 220–228. https://doi.org/10.52684/ijeska.2024.1553919

Olomo, K. O., Bayode, S., Alagbe, O. A., & Olayanju, G. M., Olaleye, O. K. (2022). Aeromagnetic mapping and radioelement influence on mineralogical composition of mesothermal gold deposit in part of Ilesha Schist Belt, Southwestern Nigeria. *NRIAG Journal of Astronomy and Geophysics, 11*(1), 177–192. https://doi.org/10.1080/20909977.2022.2057147

Ominigbo, E. O. (2022). Evolution of the Nigerian Basement Complex: Current status and suggestions for future research. *Journal of Mining and Geology, 58*(1), 229–236.

Pires, A. C. B. (1995). Identificação geofísica de áreas de alteração hidrotermal, Crixás–Guarinos, Goiás. *Brazilian Journal of Geology, 25*(1), 61–68.

Rahaman, M. A. (1988). Recent advances in the study of the Basement Complex of Nigeria. In P. O. Oluyide et al. (Eds.), *Precambrian geology of Nigeria* (pp. 11–41). Geological Survey of Nigeria.

Salako, K. A., Adetona, A. A., Rafiu, A. A., Augie, A. I., Jimoh, M. O., Alkali, A., Muriana, R. A., & Lawrence, J. O. (2024). Integrated geophysical investigation for gold mineralization potential over southern parts of Kebbi State and its environs, northwestern Nigeria. *Heliyon, 10*, e34093. https://doi.org/10.1016/j.heliyon.2024.e34093

Saleh, A., Udensi, E. E., Salako, K. A., & Unuevho, C. I. (2022). Delineation of airborne magnetic and radiometric structures associated with gold mineralization of Minna and its environs, North-central Nigeria. *Earth Sciences Pakistan (ESP), 6*(2), 54–59. https://doi.org/10.26480/esp.02.2022.54.59

Sanusi, S. O., & Amigun, J. O. (2020). Structural and hydrothermal alteration mapping related to orogenic gold mineralization in part of Kushaka Schist Belt, North-central Nigeria, using airborne magnetic and gamma-ray spectrometry data. *SN Applied Sciences, 2*, 1591. https://doi.org/10.1007/s42452-020-03435-1

Saunders, D. F., Terry, S. A., & Thompson, C. K. (1987). Test of national uranium resource evaluation gamma-ray spectral data in petroleum reconnaissance. *Geophysics, 52*(11), 1547–1556.

Sheikhrahimi, A., Pour, A. B., Pradhan, B., & Zoheir, B. (2019). Mapping hydrothermal alteration zones and lineaments associated with orogenic gold mineralization using ASTER data: A case study from the Sanandaj-Sirjan Zone, Iran. *Advances in Space Research, 63*(10), 3315–3332. https://www.sciencedirect.com/science/article/pii/S0273117719300559

Yakubu, M., Wulo, I. B., Abdullahi, J., Gazali, A. K., Lawan, Z. A., & Kamale, H. I. (2022). Geomorphometric and terrain analysis of the Nigerian section of the Chad Basin (*Bornu Basin*), Northeastern Nigeria. *Journal of Geography and Geology, 11*(4), 1–15. https://doi.org/10.5539/jgg.v11n4p1

Peer-review history:
The peer review history for this paper can be accessed here:
https://pr.sdiarticle5.com/review-history/145402